

RECENT TRENDS IN BEAM SIZE MEASUREMENTS USING THE SPATIAL COHERENCE OF VISIBLE SYNCHROTRON RADIATION

T. Mitsuhashi, KEK, Tsukuba, Japan

Abstract

The optical method of measuring the transverse beam profile and size using visible synchrotron radiation (SR) began with simple imaging systems. The resolution was limited by both diffraction and wavefront errors making it difficult to resolve beam sizes less than 50 μm . Instead of imaging, an interferometric method for measuring the beam profile and size using spatial coherence was introduced. The method is based on Van Cittert-Zernike's theorem, and can resolve 4-5 μm beam sizes with an error of only 0.5 μm . In this presentation, the principle of the measurement, the SR interferometer design, and some recent measurement results are reviewed. The incoherent field depth effect for the horizontal beam size measurement is also described with some recent results. Design study calculations for the SR interferometer at the LHC will be presented.

INTRODUCTION

The synchrotron radiation (SR) monitor based on visible optics is one of the most fundamental diagnostic tools in high energy accelerators. The monitor gives a static and dynamic observation for the visible beam profile, beam size and with a streak camera, the longitudinal profile. These diagnostics greatly improve the efficiency of commissioning and operation of the accelerator. The discipline of monitoring began with simple imaging systems [1]. The resolution in the imaging systems was limited by both the diffraction and wavefront errors making it difficult to resolve beam sizes less than 50 μm . Instead of imaging, a method for measuring the beam profile taking advantage of inherent spatial coherence was introduced [2].

Nowadays, the SR interferometer is recognized as a powerful tool to easily measure small beam sizes [3]. Recent efforts to improve the measurable range down to 3-4 μm have been reported [4]. In recent few years, an imbalance input technique was developed to introduce magnification into the interferometer [4][5][6]. The principal of the measurement, and some recent results are reviewed in this paper.

PRINCIPAL OF THE MEASUREMENT

In visible optics, interferometry is one of the standard methods to measure the profile or size of very small objects. The principle of measuring the profile of an object by means of spatial coherence was first proposed by H. Fizeau in 1898 [7], and is now known as the Van Cittert-Zernike theorem [8]. In other hand, it is well known that A. A. Michelson measured the angular dimension (extent) of a star with his stellar interferometer

in 1920 [9]. With interferometry, all free parameters such as wavelength distance between object and interferometer and separation of double slit are measured by interferometry and a ruler. Due to this self-consistently, this method is classified as an *absolute* measurement.

Considering an incoherent light source as an ensemble of the single, independent modes of the emitted light, according to the van Cittert-Zernike theorem, the intensity distribution of the object is given by the Fourier transform of the complex degree of 1st order spatial coherence [8]. Mathematically, if we let f denotes the two dimensional transverse intensity distribution of beam profile as a function of coordinates x, y , the 1st order complex degree of spatial coherence γ as a function of spatial frequency ν_x and ν_y is given by ,

$$\gamma(\nu_x, \nu_y) = \int f(x, y) \exp\{-2\pi i(\nu_x x + \nu_y \cdot y)\} dx dy$$

$$\nu_x = \frac{2\pi D_x}{\lambda R}, \nu_y = \frac{2\pi D_y}{\lambda R} \quad (1)$$

where R denotes the distance between the source and the double slit. We can therefore obtain the beam profile and thus beam size via the inverse Fourier transform of complex degree of 1st order spatial coherence as measured with a 2-slit interferometer.

SR INTERFEROMETER

In order to measure the 1st order spatial coherence of a SR beam, a wavefront-division type interferometer using polarized, quasi-monochromatic rays is used. An outline of the interferometer is shown in Fig. 1 [2][3].

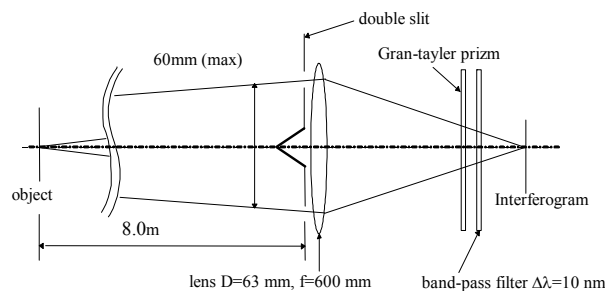


Figure 1: Outline of the 2 slit wavefront-division type of SR interferometer.

A diffraction-limited high quality lens (such as ED apochromat) is used to focus the beam onto the screen. In the vertical plane, there exists a π phase difference between the interference fringes relative to the σ -polarized fringes [2]. A Gran-Taylor prism is used to select the σ component of the SR. A band-pass filter is used for obtain quasi-monochromatic light. An eyepiece

Content from this work may be used under the terms of the CC BY 3.0 licence (© 2015). Any distribution of this work must maintain attribution to the author(s), title of the work, publisher, and DOI.

toshiyuki.mitsuhashi@kek.jp

lens is applied for further magnification of the interferogram for the convenience of observation and an image sensor such as CCD is used to observe the interferogram.

With the SR interferometer, the intensity of the interferogram for the vertical plane is given by,

$$I(y,D) = \int \zeta(\lambda) \cdot (I_1 + I_2) \cdot \left\{ \text{sinc} \left(\frac{\pi \cdot \alpha \cdot y \cdot \zeta(D)}{\lambda \cdot f} \right) \right\}^2 \cdot \left\{ I + \gamma \cdot \cos \left(k \cdot D \cdot \left(\frac{y}{f} + \psi \right) \right) \right\} d\lambda$$

$$\gamma = \left(\frac{2\sqrt{I_1 \cdot I_2}}{I_1 + I_2} \right) \cdot \left(\frac{I_{\max} - I_{\min}}{I_{\max} + I_{\min}} \right), \quad (2)$$

where y denotes vertical position on the observation plane, a denotes the half-height of the slit, $\zeta(\lambda)$ denotes the spectral properties of the band-pass filter, D denotes double slit separation and f denotes the distance between back principal point of the lens and the interferogram. γ is the visibility of the interferogram.

In the horizontal plane, the interferogram includes the additional effect of incoherent depth of field (IDOF) by the instantaneous opening of the SR [3] in the horizontal plane. The IDOF has two effects, the first is the apparent horizontal beam size becomes bigger and the second is the visibility of the horizontal interferogram reduces by intensity imbalance at two opening of double slit. If we represents the instantaneous intensity distribution of SR in horizontal plane by $I(\theta)$ as a function of horizontal observation angle θ , the apparent beam shape $\sigma_a(x)$ including the intensity imbalance factor is given by [3],

$$\sigma_a(x) = \int \frac{2\sqrt{I\left(\theta + \frac{D}{2R}\right)I\left(\theta - \frac{D}{2R}\right)}}{I\left(\theta + \frac{D}{2R}\right) + I\left(\theta - \frac{D}{2R}\right)} \cdot I(\theta) \cdot \frac{\exp\left[-\frac{[x - \rho\{1 - \cos(\theta)\}]^2}{2\sigma^2}\right]}{\sigma \cdot \sqrt{2\pi}} d\theta \quad (3)$$

where the original beam profile is assumed to be a Gaussian. The visibility of the interferogram $\gamma_h(D)$ is given by Fourier cosine transform of the apparent beam shape as follows,

$$\gamma_h(D) = \int \sigma_a(x) \cdot \cos\left(\frac{2\pi \cdot D \cdot x}{R \cdot \lambda}\right) dx \quad (4)$$

For a detailed explanation of the horizontal instantaneous SR opening angle and IDOF effect on horizontal beam size interferometry, see references [3] and [10].

SMALL BEAM SIZE MEASUREMENT BY USING A GAUSSIAN BEAM PROFILE

We can often approximate the beam profile with a Gaussian shape. Under this approximation, we can obtain the RMS beam size from the measured visibility at a fixed separation D of the double slits. With this method the RMS beam size σ_{beam} is given by,

$$\sigma_{\text{beam}} = \frac{\lambda \cdot F}{\pi \cdot D} \cdot \sqrt{\frac{1}{2} \cdot \ln\left(\frac{1}{\gamma}\right)} \quad (5)$$

where γ denotes the visibility [3]. This method does not require measuring the visibility as a function of the slit

separation. The method is suitable to measure a small beam size in which we can approximate the beam profile with a Gaussian distribution.

THEORETICAL AND PRACTICAL RESOLUTION AND ERROR

According to quantum optics theory, the following uncertainty principle hold [11],

$$\Delta\phi \cdot \Delta n \geq \frac{1}{2} \quad (6)$$

where $\Delta\phi$ and Δn are the uncertainties of the photon phase and the photon number, respectively. The visibility of interferogram will therefore smear in the following manner [4],

$$I(y,D) = (I_1 + I_2) \cdot \left\{ \text{sinc} \left(\frac{\pi y}{\lambda f} \right) \right\}^2 \cdot \left\{ 1 + \int_{\Delta\phi} \cos(kD \frac{y}{f} + \phi) \xi(\phi) d\phi \right\} \quad (7)$$

where $\xi(\phi)$ denotes probability distribution function for phase. But, in practice, we use a sufficient number of photons for the interferometry, the theoretical limit for the resolution due to the phase uncertainty is very small, and not observable (for example, 10^4 photons corresponds 0.5×10^{-4} rad, and the visibility is sufficiently equal to unity).

The instrumental error due to the Optical components is also important. Using good quality optical components, such as lens having a peak-to-valley wavefront error better than $\lambda/10$ can produce the object size error to about $0.26 \mu\text{m}$ in the interferometer at the ATF.

In addition, the statistical noise in image sensor can influence the measurement [4]. The error $\Delta\gamma$ in visibility transfers into a beam size error $\Delta\sigma$ by,

$$\Delta\sigma = \frac{\lambda \cdot F}{\pi \cdot D} \cdot \frac{1}{\gamma \cdot \sqrt{8 \cdot \ln\left(\frac{1}{\gamma}\right)}} \cdot \Delta\gamma \quad (12)$$

A γ dependence of error transfer from $\Delta\gamma$ to $\Delta\sigma$ for the condition $\Delta\gamma=0.01$ is shown in Fig. 19. The experimental setup of ATF is applied in this calculation. As seen in Fig. 2, there exists a significant error enhancement in the range γ larger than 0.95.

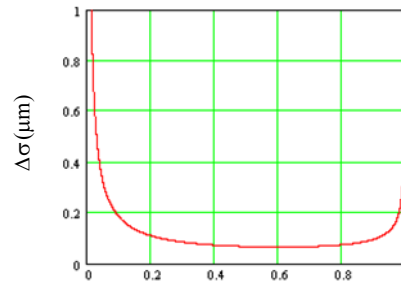


Figure 2: Error transfer from $\Delta\gamma$ to $\Delta\sigma$ assuming $\Delta\gamma=0.01$ as a function of γ .

To see this tendency, the beam size measured by changing the double slit separation at ATF is shown in Fig. 3 [4].

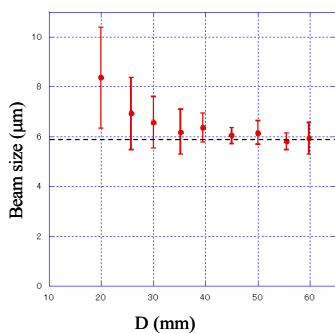


Figure 3: Apparent increase of the beam size with separation range of the double slit. $D=40\text{mm}$ corresponds to $\gamma=0.864$.

From Fig. 3, an apparent systematic increase of beam size is observed in the double slit separation range smaller than 35 mm in which the visibility of the interferogram exceeded 0.9, due to non-linearity near the baseline of CCD camera. The statistical error is increased in smaller D range. The visibility 0.90 with $D=60\text{ mm}$, $\lambda=400\text{ nm}$ for the ATF interferometer corresponds to a beam size of $3.5\text{ }\mu\text{m}$. This size seems smallest measurable size with a normal setup of the interferometer.

Since the measurement is still not limited theoretically, an intensity imbalance on the two slits can be introduced to reduce the systematic and the statistical errors on the CCD. For details of this method, please see reference [4] and [5]. Mechanical vibration is also significant to interferometry, but will not be covered in this paper. Please see reference [3].

MEASUREMENT OF VERTICAL SMALL BEAM SIZES

Recent interferometry on the vertical beam size measurements are introduced here. Vertical slit scan measurements at ALBA and SPEAR3, and small vertical beam size measurements using the Eq. (5) at SPEAR3 and ATF is discussed.

Slit Scan Measurements at ALBA and SPEAR3

An example of a high-visibility interferogram measured at ALBA is shown in Fig 4.

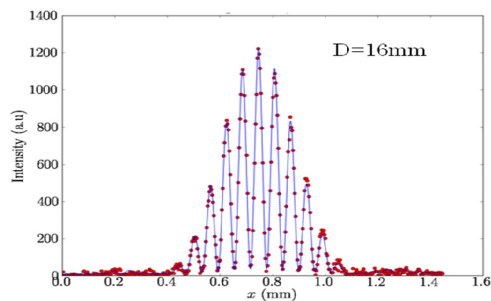


Figure 4: High visibility vertical interferogram measured at ALBA. $D=16\text{ mm}$, $\lambda=538\text{ nm}$.

This interferogram was measured with double slit separation of 16mm and a wavelength of 538 nm. The visibility as a function of double slit separation is shown in Fig. 5. The data shows the measured visibility very Gaussian, and the concluded RMS vertical beam size was $22.5\text{ }\mu\text{m}$.

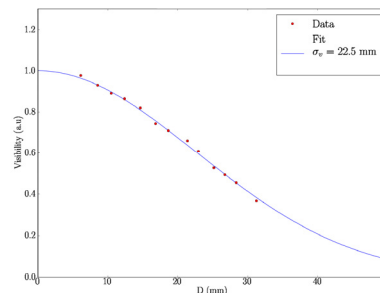


Figure 5: Visibility as a function of double slit separation at ALBA. Solid blue line is the Gaussian fitted result.

The next example is comes from SPEAR3. The result of an interferogram measured with double slit separation of 70 mm and wavelength of 550 nm is shown in Fig. 6 [12]. The visibility as a function of double slit separation is shown in Fig. 7 [12].

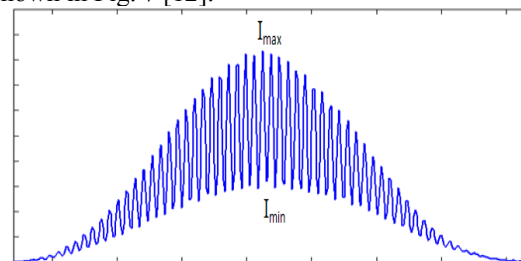


Figure 6: Typical interferogram at SPEAR3. $D=70\text{ mm}$
 $\lambda=550\text{ nm}$.

The concluded RMS vertical beam size was $23.2\text{ }\mu\text{m}$.

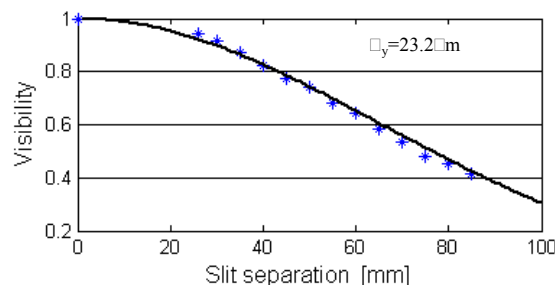


Figure 7: Visibility as a function of double slit separation at SPEAR3. The dotted line is measurement result, and the solid line is a Gaussian fit.

Content from this work may be used under the terms of the CC BY 3.0 licence (© 2015).

Small Beam Size Measurement Using the Eq. (5) at SPEAR3 and the ATF

Figures 5 and 6 show the measured spatial coherence as a function of slit separation has a Gaussian distribution for the stored beam in the equilibrium state. This result indicates the beam profile has a Gaussian distribution. Assuming a Gaussian beam profile approximation, as described in previous section, we can measure a small beam size using a single data point (Eq. (5)). In this case, for very small beam size measurement, chromatic aberration in the objective lens can introduce serious error [13]. To minimize chromatic aberrations, a Herschelian reflective optics can be applied for the interferometer as shown in Fig. 8.

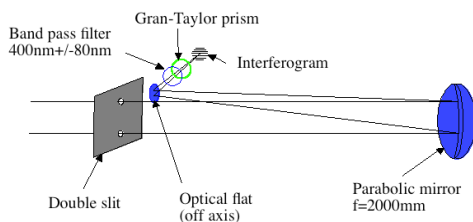


Figure 8: Herschelian reflective optics configuration.

The first example for the single-point method is again a measurement from SPEAR3. A measured interferogram at $D=50$ mm, $\lambda=550$ nm for low coupling mode operation is shown in Fig. 9. The focal length of the main mirror was chosen 1200mm to reduce digitisation errors in the CCD due to the fine pitch of the interference fringes

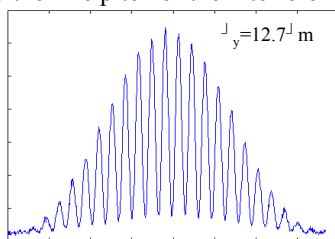


Figure 9: Interferogram measured at $D=50$ mm and $\lambda=550$ nm for low coupling mode at SPEAR3.

The resulting of beam size evaluated from the Eq. (5) from the visibility of this interferogram was $12.7 \mu\text{m}$.

The next example is a measurement performed at the ATF [13]. The focal length of the main mirror was 2000 mm to again reduce from a digitisation errors in the CCD due fine pitch of the interference fringes. In this measurement, the slit separation was 60 mm. The wavelength was 400nm and bandwidth 80 nm to obtain enough intensity. The spectral characteristic of the band-pass filter was included in the fitting. The beam obtained size from this interferogram was $4.7 \mu\text{m}$.

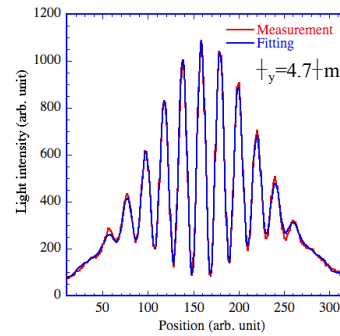


Figure 10: Interferogram at the KEK ATF. Red line is measurement, and blue line is fitting. Interferogram measured with $D=60$ mm and $\lambda=400$ nm.

HORIZONTAL BEAM SIZE MEASUREMENT

Horizontal beam size measurements are performed by using Eq. (4) which includes the incoherent depth of field effect (IDOF). Three examples for large, medium and small horizontal sizes are introduced in this section

First example is a horizontal beam size measurement at SPEAR3. The visibility as a function of the slit separation is shown in Fig. 11 [14].

Two analysis methods, one is including the IDOF and other is not including IDOF are shown in the figure. The result of horizontal beam size is $132.7 \mu\text{m}$. Due to this large horizontal beam size, the effect of IDOF is rather small.

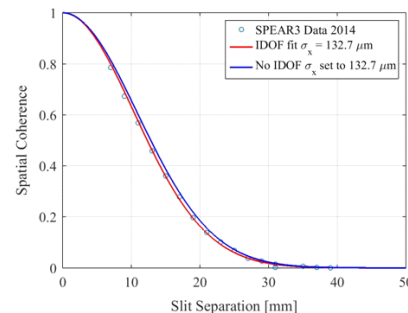


Figure 11: Horizontal beam visibility measurements at SPEAR3. Dots are measurements, red line is fitting Eq (4) and blue line is calculated visibility curve for a beam size $132.7 \mu\text{m}$ without IDOF.

The second example is a measurement made at the Australian Synchrotron ASLS [14]. The measured horizontal visibility is shown in Fig. 12 and the horizontal beam size taking IDOF into account is $88 \mu\text{m}$. Due to a smaller horizontal beam size at the source point the effect of IDOF is larger than at SPEAR3.

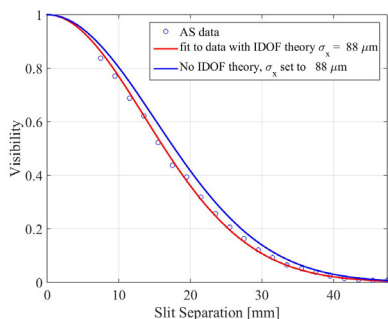


Figure 12: Horizontal visibility measured at ASLS as a function of slit separation. Dots are measurements, red line is fitting Eq (4) and blue line is calculated visibility curve for a beam size 88 μm without IDOF.

The third example is a measurement taken at the ATF [14]. The measured horizontal visibility is shown in Fig. 13 and the horizontal beam size taking IDOF into account is 38.5 μm . Due to smaller horizontal beam size, the effect of IDOF is the largest in these three examples.

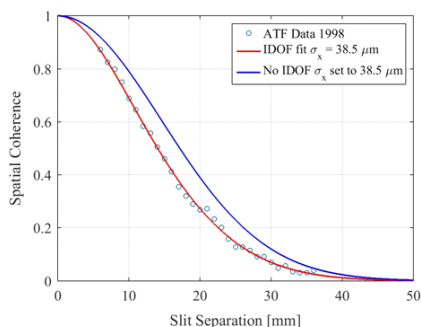


Figure 13: Horizontal visibility measured at ATF as a function of slit separation. Dots are measurements, red line is fitting Eq (4) and blue line is calculated visibility curve for a beam size 38.5 μm without IDOF.

In each case the results for horizontal beam size measurements are in good agreement with designed values when the IDOF effect is taken into account.

BEAM SIZE INTERFEROMETRY MEASUREMENT AT THE LHC

In the past for the SR monitor at LHC, a simple imaging system has been applied to measurement of the beam profile [15]. To produce the visible SR component at the injection energy (450 GeV), a superconducting 2-period undulator was installed. Edge radiation from a bending magnet is used at medium energy, and SR from the core bending magnet is used for high energy. Due to thermal deformation and diffraction extraction mirror problems, no reliable result for the beam size has been obtained from the imaging system.

To improve this situation, a beam size measurement system based on an interferometer has been designed for

the LHC upgrade project [16,17]. Due to a very long dipole magnet bending radius and a rather narrow opening angle for the SR, a large IDOF effect is expected for the horizontal beam size measurement. Since the undulator has no IDOF, no such a problem is existing in the beam size measurement at the injection energy. The expected visibility as a function of double slit separation for designed beam size of 1.12 mm at 450 GeV is shown in Fig. 14 (a). The expected visibility for designed beam size of 0.33 mm at 5 TeV and 0.28mm at 7 TeV are shown in Figures 14 (b) and (c), respectively. Compared to the visibility curve at 450GeV, the visibility curves in the high energy region are expected to have a large IDOF.

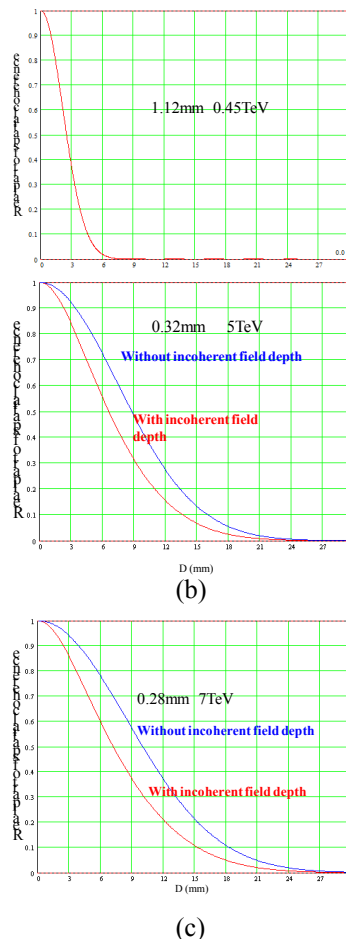


Figure 14: Calculated visibility curves as a function of double slit separation at the LHC. (a) beam size of 1.12 mm at 450 GeV. (b) beam size of 0.33 mm at 5 TeV and (c) beam size of 0.28 mm at 7 TeV

The optical beam lines on the diagnostic table will be rearranged to add the new interferometer system. The interferometry will start with the vertical direction because it is simpler than the horizontal measurement. A test interferometer for vertical measurement has been installed for operation of the LHC in 2015, and awaiting first light.

Content from this work may be used under the terms of the CC BY 3.0 licence (© 2015). Any distribution of this work must maintain attribution to the author(s), title of the work, publisher, and DOI.

SUMMARY

The introduction to measurement principle, van Cittert-zernike's theorem, the design of SR interferometer and interferograms for vertical and horizontal is discussed. The theoretical resolution and the practical errors are also discussed, which indicate we can measure the vertical beam size down to 3-4 μm . Recent trends in measurements for vertical and horizontal beam sizes in ALBA, SPEAR3, ASLS and ATF were reviewed. As a fresh topic, SR interferometry for LHC was also introduced. The beam size measurement with SR interferometry is getting popular not only for electron machines, but also for high-energy the proton machines such as the LHC.

ACKNOWLEDGMENT

The author would like to acknowledge Dr. Ubaldo Iriso and Miss. Laura Trino of ALBA, Dr. Mark Boland of ASLS and Dr. Jeff Corbett of SLAC for providing the measurement results and helpful discussions. The author also thanks to Drs. Federico Roncarolo, Enrico Bravin and Gerges Trad for providing the LHC information and helpful discussions

REFERENCES

- [1] T. Mitsuhashi and M. Kato, Proc. 5th European Particle Accelerator Conf. 1669 (1996).
- [2] Mitsuhashi, Proc. of 1997 Particle Accelerator Conference, 766 (1997) Vancouver.
- [3] T. Mitsuhashi, "Beam Profile and Size Measurement by SR Interferometer" in Beam measurement, Ed. by S. Kurokawa et al., 399-427, World Scientific (1999).

- [4] T. Naito and T. Mitsuhashi, Proc. of IPAC'10, 972 (2010) Kyoto.
- [5] T. Mitsuhashi, Proc. of IBIC2012, 576 (2012) Tsukuba.
- [6] M. Boland et al., Proc. of IBIC2012, 566 (2012) Tsukuba.
- [7] H. Fizeau, C.R. Acad. Sci. Paris, 66, 934 (1868).
- [8] P. H.van Cittert, *Physica*, 1, 201 (1934). See also F. Zernike, 'The Concept of Degree of Coherence and Application to Optical Problems', *Physica*, Vol. 5, (1938).
- [9] A. A. Michelson, *Astrophysic. J*51, 257 (1920).
- [10] T. Mitsuhashi, "lecture note for ASLS school for accelerator physics 2014," in <https://accelerators.org.au/asap2>
- [11] For example, see R. Loudon *Quantum Theory of Light*", Oxford University Press (1983).
- [12] J. Corbett et al., Proc. Particle Accelerator Conference, 4018 (2009) Vancouver.
- [13] T. Naito and T. Mitsuhashi, *Phys. Rev. ST Accel. Beams* 9, 122802 (2006).
- [14] M. Boland et al., TUPWA001, Proc. IPAC'15.
- [15] A. S. Fisher, Expected Performance of the LHC Synchrotron-light Telescope (BSRT) and Abort-Gap Monitor (BSRA)," tech. rep., 2010, 49, 51, 80, 120.
- [16] A. Goldblatt, E. Bravin, F. Roncarolo, and G. Trad, Proc. of IBIC 2013, 220 (2013) Oxford.
- [17] G. Trad, Phd thesis, Grenoble University (2015).